

RECEIVED: September 14, 2011

REVISED: November 15, 2011

ACCEPTED: December 18, 2011

PUBLISHED: January 5, 2012

# Room temperature spectroscopy of deep levels in junction structures using barrier capacitance charging current transients

**E. Gaubas,<sup>a,1</sup> T. Ceponis,<sup>a</sup> A. Uleckas<sup>a</sup> and R. Grigonis<sup>b</sup>**

<sup>a</sup>*Vilnius University, Institute of Applied Research,  
Sauletekio al. 9-III, LT-10222, Vilnius, Lithuania*

<sup>b</sup>*Vilnius University, Laser Research Centre,  
Sauletekio al. 10, LT-10223, Vilnius, Lithuania*

*E-mail:* [eugenijus.gaubas@ff.vu.lt](mailto:eugenijus.gaubas@ff.vu.lt)

**ABSTRACT:** A technique is presented for room temperature spectroscopy of deep levels in semiconductor devices based on measurements of current transients due to barrier capacitance charging. Spectroscopic measurements are obtained from a set of the barrier capacitance charging current transients modified by illumination pulses with wavelength between 1.5 and 10  $\mu\text{m}$ . Deep levels with activation energy in the range between 0.24 and 0.56 eV have been revealed in thyristor and neutron irradiated particle detector structures by using this technique.

**KEYWORDS:** Radiation damage evaluation methods; Detection of defects; Solid state detectors

---

<sup>1</sup>Corresponding author.

---

## Contents

<b>1</b>	<b>Introduction</b>	<b>1</b>
<b>2</b>	<b>Principles of photo-ionization probing by barrier capacitance charging transients</b>	<b>1</b>
<b>3</b>	<b>Samples and measurement instrumentation</b>	<b>4</b>
<b>4</b>	<b>Illumination dependent barrier capacitance charging current transients</b>	<b>5</b>
<b>5</b>	<b>Illumination spectrum dependent BELIV current transients in the irradiated diodes</b>	<b>7</b>
<b>6</b>	<b>Summary</b>	<b>8</b>

---

## 1 Introduction

Deep level transient spectroscopy is traditionally used to characterize deep levels in semiconductors by measuring changes of either capacitance [1, 2] or current [3]. Common measurement regimes include either temperature scans or low temperature experiments, when only processes of carrier emission from deep levels are controlled. Photo-ionization spectroscopy [4] can be an alternative tool with the advantage that the measurements can be performed at room temperature. In this work, a technique for spectroscopy of deep levels within junction device structures based on measurements of barrier capacitance charging current transient changes due to additional spectrally resolved pulsed illumination is proposed. This technique allows for the simultaneous monitoring of the changes of excess carrier capture and short emission lifetime based on spectrally varied deep level filling/emptying in junction structures of semiconductor devices.

## 2 Principles of photo-ionization probing by barrier capacitance charging transients

The Barrier Evaluation (BELIV) [5]–[7] technique for a reverse biased junction is based on analysis of the changes of barrier capacitance ( $C$ ) with linearly increasing voltage (LIV)  $U_p(t) = At$  pulse. To present the principles of the BELIV-IR (infrared) pulsed spectroscopy technique, a common depletion approximation [1] is applied. Then, the barrier capacitance  $C(t) = \epsilon\epsilon_0 S/W(t)$  temporal ( $t$ ) changes under LIV pulse in n-type junction layer is ascribed (within this simplified approach) to variation of a depletion width

$$W(t) = \left[ \frac{2\epsilon\epsilon_0(U_{bi} + At)}{e(N_D + (N_d - n_d(t)))} \right]^{1/2}. \quad (2.1)$$

Here  $\epsilon_0$  is the vacuum dielectric constant,  $\epsilon$  the material permittivity,  $e$  the elementary charge,  $S$  the junction area,  $U_{bi}$  the built-in potential barrier,  $N_D$  the shallow dopants density,  $N_d$  the density of

deep donor type traps,  $n_d$  the concentration of electrons trapped on  $N_d$ , and  $A = U_P/\tau_P$  the ramp of the LIV pulse with amplitude  $U_P$  and of duration  $\tau_P$ . Without additional IR illumination, the time dependent changes of the charge  $q = CU$  within the junction, determine the current transient  $i_C(t)$ :

$$i_C(t) = \frac{dq}{dt} = \frac{d[C(t)U(t)]}{dt} = AC(t) \left[ \frac{1 + \frac{At}{2U_{bi}}}{1 + \frac{At}{U_{bi}}} + \frac{t}{2\tau_{gd}} \frac{n_d(t)}{N_D + (N_d - n_d(t))} \right]. \quad (2.2)$$

This transient contains the displacement and conductivity current components. The latter component arises within transitional layer (due to free carrier “tail”) at depletion boundary (for a more rigorous approach of extended depletion approximation, see [1]) caused by prevailing of carrier thermal generation (from  $N_d$  traps) with increase of the depletion width  $W(t)$  under reverse bias LIV. Here, it is assumed that trapped (at  $N_d$ ) carriers are released according to  $n_d(t) = n_{d0}\exp(-t/\tau_{gd})$ , with steady-state ( $N_d$  filling) concentration  $n_{d0}$ . The thermal generation lifetime  $\tau_{gd} = 1/[\sigma_{dth}v_T N_C \exp(-E_d/kT)]$  is a function of the emission cross-section  $\sigma_{dth}$ , of the thermal velocity  $v_T$ , of the density of states in the conductivity band  $N_C$ , and of activation ( $E_d$ ) as well as of thermal ( $kT$ ) energy. As usually, several trap species of different types appear. Generation currents from slower and deeper traps contribute simultaneously to the leakage current, which is expressed as  $i_{gl}(t) = en_i W(t) S / \tau_{gl}$ , through the averaged lifetime  $\tau_{gl}$  as well as through intrinsic carrier density  $n_i$ .

At room temperature, values of carrier thermal generation lifetimes, even for moderately deep ( $E_i < E_d < E_C$ ) donor-type centres in Si, appear to be in the range from a few  $\mu s$  to ns (figure 1a) for traps with  $\sigma_{dth}$  in the range of  $10^{-14}$ – $10^{-16}$  cm<sup>2</sup>. Therefore, only traps with short carrier capture lifetimes ( $\tau_{Cd}/\tau_{gd} < 1$ ) can be filled. Carrier capture lifetime  $\tau_{Cd}$  is a reciprocal function of the trap density,  $N_d$ :  $\tau_{Cd} = 1/\sigma_{dth}v_T N_d$ . Thus, impact of generation current ascribed to the single type traps can be observable as an initial recess within the BELIV transients when density of these traps approaches to or exceeds the concentration  $N_D$  of shallow dopants. The simulated (using eq. (2.2)) BELIV transients (curves 1–3) obtained varying  $n_{d0}$  are illustrated in figure 1b. It can be noticed in figure 1b, that initial recess within the barrier charging current transient is observed when rather large density of initially filled traps exists. In the opposite case, when several species of traps compete in capturing free carriers, only partial and rather low filling of these traps is possible (carriers of low density are redistributed among different traps). Then, generation-leakage current  $i_{gl}$  increases with  $At$  voltage and can exceed the barrier charging current in the rearward phase of the transient. The descending charge extraction (displacement current) component and the ascending generation  $i_{gl}$  current component imply the existence of a current minimum in the current transient [5], which can be highlighted using increased LIV pulse duration.

Photo-ionization of trapped carriers  $n_d$  by using short (fs) pulses of spectrally well resolved IR light enables one to determine parameters of deep traps and state of their filling. Short IR pulse with incident  $h\nu$  energy photons of surface density  $F(h\nu)$  integrated per pulse duration makes  $\delta$ -shape ( $\sim 0.2$  ps within scale of BELIV  $\mu s$  pulses) optical emission of trapped carriers, if  $h\nu$  fits to  $E_d$  and cross-section  $\sigma_{p-e}$  of photon-electron interaction is sufficient. The cross-section  $\sigma_{p-e}$  for electrons located in deep levels is widely [1, 4] described by Lucovsky model [8]:

$$\sigma_{p-e}(h\nu) = \frac{BE_d^{1/2}(h\nu - E_d)^{3/2}}{(h\nu)^3}, \quad (2.3)$$

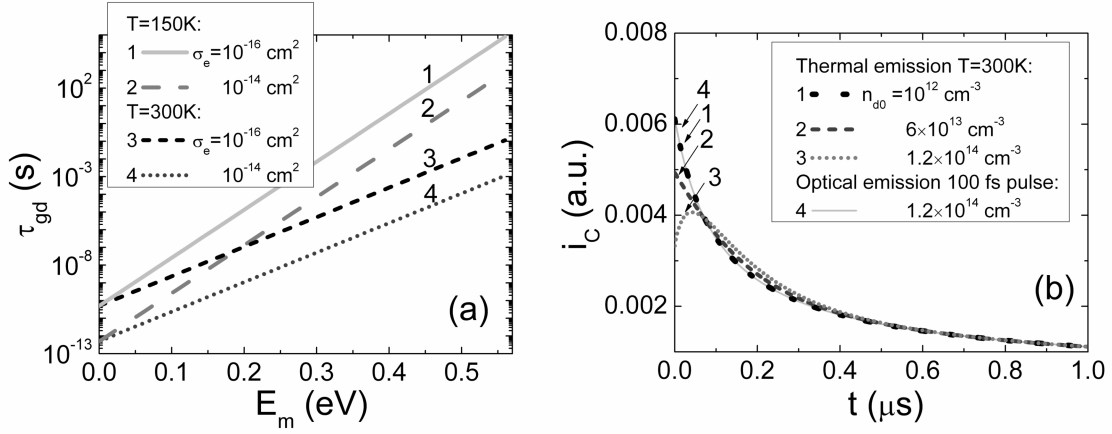


**Figure 1.** a- Simulated thermal emission lifetimes at 150 (1,2) and 300 K (3,4) temperatures for traps with emission cross-section  $\sigma_e = 10^{-16} \text{ cm}^2$  (1,3) and  $\sigma_e = 10^{-14} \text{ cm}^2$  (2,4), respectively. b- Simulated barrier ( $N_D = 7 \times 10^{13} \text{ cm}^{-3}$ ) charging current transients when carriers of different density  $n_{d0}$  trapped at deep donor centres ( $N_d = 1.2 \times 10^{14} \text{ cm}^{-3}$ ) are released thermally (1–3 curves) and by short IR light pulse (4).

where  $B$  is a multiplicative factor. The spectral changes of the absorption coefficient  $\alpha(h\nu)$  due to photo-ionization can be described by

$$\alpha(h\nu) = \sigma_{p-e}(h\nu)n_{d0}. \quad (2.4)$$

This change of the absorption coefficient can be controlled by  $h\nu$  light induced transmission measurements. IR induced absorption measurements are performed in nearly wave-guide regime within layered device structures. Illumination by IR light pulse of surface density  $F(h\nu)$  leads to density of photo-emitted carriers:

$$n_d^* = \sigma_{p-e}(h\nu)n_{d0}F(h\nu). \quad (2.5)$$

By substituting  $n_d^*$  (eq. (2.5)) (with  $n_d^* = n_d(t)$ ), into eq. (2.2), a value for the barrier capacitance charging current due to photo-ionization can be extracted. The simulated (using eqs. (2.2) and (2.5)) BELIV transient (curve 4) is illustrated in figure 1b. Density of the photo-excited carriers  $n_d^*$  by  $h\nu$  light pulse can be independently controlled by using contactless microwave probed photoconductivity transients [9]. Then, density of  $N_d$  traps can be extracted using eq. (2.2), if doping density  $N_D$  is known. The filling factor  $n_d/N_d$  can be controlled by combined measurements of  $i_c$  peak value or  $\alpha(h\nu)$  (as well as  $n_d^*$ ) as a function of  $F|_{h\nu}$ , and saturation of these characteristics indicates complete photo-ionization of  $N_d$  traps. Generation current parameters can be extracted by combined analysis of the BELIV current transients measured with and without IR illumination. Photo-ionization within electrically neutral region leads to a reduction of the dielectric relaxation time and of the serial resistance in the junction structure. The enhanced density of excess carriers within electrically neutral region decreases duration of the initial rise to peak current, as discussed elsewhere [6], and results in thinner Debye length of the transitional layer nearby depletion boundary.

Activation energy  $E_d$  of  $N_d$  traps can be evaluated by spectral measurements of changes in BELIV current transient shape and initial peak amplitude and using eqs. (2.3)–(2.5). These spectral measurements are as usually started from the long wavelength wing to avoid simultaneous trap

filling/emission from deeper centres. Value of  $E_d$  can be evaluated as quantum energy  $h\nu$  or which the red-threshold of the IR modified  $i_C$  increase is observed. Alternatively,  $E_d$  and  $\sigma_{p-e}(h\nu)$  can be estimated by combining simulations of the BELIV current amplitudes based on eqs. (2.2)–(2.5).

The simplified description of principles of the technique of photo-ionization probed barrier capacitance charging transients is presented above by analyzing the donor type traps. Both acceptor and donor type defects acting together can be found in real experimental practice. Analysis of such models (when acceptors behave like compensating centres, while donors are able to follow fast changes in pulsed voltage) could be found e.g. in monograph [1]. The BELIV-IR (infrared) pulsed spectroscopy technique is preferential to evaluate material characteristics at room temperature when density of traps is large. However, an impact of the electron-phonon interactions within room-temperature photo-ionization spectroscopy should be estimated. In high resistivity materials, deep traps of high density are partially filled due to lack of free carriers. Then, generation current prevails in BELIV transients. Next section illustrates examples of applications of the above technique with Si structures where defects are present either as contaminants or as radiation-induced microscopic damage.

### 3 Samples and measurement instrumentation

The BELIV-IR (infrared) pulsed spectroscopy technique was applied to analysis of deep level spectra in the Si thyristor and pin detector structures. Industrial non-capsulated Si thyristor  $n^+pnp$  structures with well defined layer thicknesses and doping ( $N_D = 7 \times 10^{13} \text{ cm}^{-3}$ , phosphorus doped n-layer) densities were used for recording deep level spectra in a  $350 \mu\text{m}$  thick n-Si layer. The tentative measurements on deep level transient spectroscopy (C-DLTS) in these  $n^+/pnp$  structures showed technological contaminants of significant density within n-layer. Also, a set of pin diodes of CERN standard  $p^+nn^+$  detector structure (with dopants density of  $N_D \cong 10^{12} \text{ cm}^{-3}$  in n-Si layer of  $\sim 300 \mu\text{m}$  thickness) irradiated by reactor neutrons with fluences in the range of  $10^{12}$ – $10^{16} \text{ n/cm}^2$  was investigated. The characteristics of the deep level filling/emptying processes over space charge and electrically neutral ranges within the high resistivity junction layer were measured by recording barrier capacitance charging and generation current transient changes [5]–[7].

A schematic representation of the measurement set-up is shown in figure 2. A pulsed illumination with variable wavelength light was provided using a differential frequency generator (DFG) coupled with an optical parametric oscillator (OPO). The OPO-DFG laser system enables to vary the illumination wavelength ( $\lambda$ ) in the range between  $1.2$  and  $10 \mu\text{m}$  with a precision of  $100 \text{ nm}$  using  $100 \text{ fs}$  pulses of the main coupling laser (CL). The triggering system of the main laser also generates synchronization pulse which starts the LIV generator (GLIV) through a synchronization pulse generator (SPG). The SPG forms a pulse of suitable duration to handle the sequence of LIV pulses and, thus, the optical (OPO-DFG) and electrical (LIV) pulses are synchronized. The OPO-DFG illumination of the device under test (DUT) leads to photo-ionization of carriers from the filled deep traps. The pulsed light biasing has been used to modify the occupation of the trap states and to highlight the dominant components of current. The illumination wavelength range of  $2$  to  $10 \mu\text{m}$  determines a monopolar excess carrier generation (as sketched in the inset of figure 3), which causes both a generation current ( $i_{gl}$ ) within the space charge region (SCR) of the junction and a monopolar photoconductivity within the electrically neutral region (ENR). The cur-

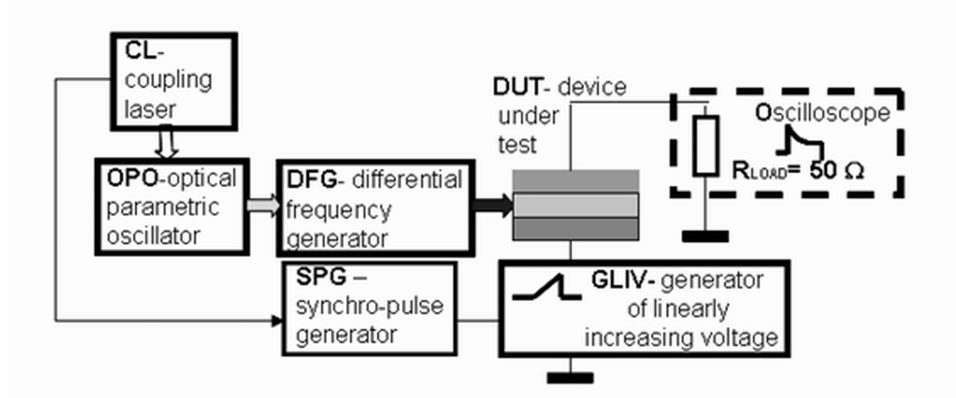


**Figure 2.** Schematic representation of the measurement set-up.

rent changes due to photo-ionization are analyzed by controlling the shape and the amplitude of the barrier capacitance charging current (BCC) transients. These BCC transients are registered using a  $50\ \Omega$  load input of a DSO6102A oscilloscope. Additionally, the measurement circuitry contains the adjustable output of a generator of linearly increasing voltage (GLIV) and the device under test (DUT), connected in series. The other channel of the digital oscilloscope is used for synchronous control of the linearity of the GLIV signal using a signal differentiating procedure installed in the DSO oscilloscope.

#### 4 Illumination dependent barrier capacitance charging current transients

For an n-layer containing a high density of deep traps, the BCC transient (**A**- and **C**-type transients illustrated in figure 3a) contains an initial recess. This recess within a BCC transient indicates a reduced  $AC(t \cong 0)$  barrier charging current due to trap filling. It can be seen in figure 3a (**B**-type transients), that an illumination pulse of fixed density and at a fixed wavelength ( $\lambda = 4\ \mu\text{m}$ ) restores the initial peak associated with the barrier charging current. This happens when emptying of the carrier capture donor-type centres in the material is saturated by a sufficient density of illumination ( $F(h\nu)$ ). Due to the emptied centres, the initial recess disappears in the BELIV transient. It can be also inferred that the value of the carrier capture lifetime determines the relaxation of the value of the initial current peak associated with the barrier charging (figure 3a, **B**-type transients). The photoconductivity current can be additionally estimated by analysis of the pedestal signal between the sequences of transients of **B**-type. The amplitude of this pedestal signal decreases together with that of the BCC signal. The evolution of BCC transients illustrated in figure 3 is obtained only for fixed wavelengths of IR illumination.

Varying the wavelength of this OPO-DFG IR pulsed illumination, a spectrum of deep levels is obtained. Additional measurements of the capacitance voltage (C-V) and current-voltage (I-V) characteristics on thyristor structures, by separately connecting the different junctions of the structures to a measurement circuitry and by using the same samples, indicated a large leakage current. The capacitance dependence on the ac test signal frequency suggests that the characteristic lifetimes of carrier capture are of the order of magnitude  $\sim 1\ \mu\text{s}$ . This is directly corroborated by the analysis of the shape of BCC transients observed for different intensities of the OPO-DFG IR

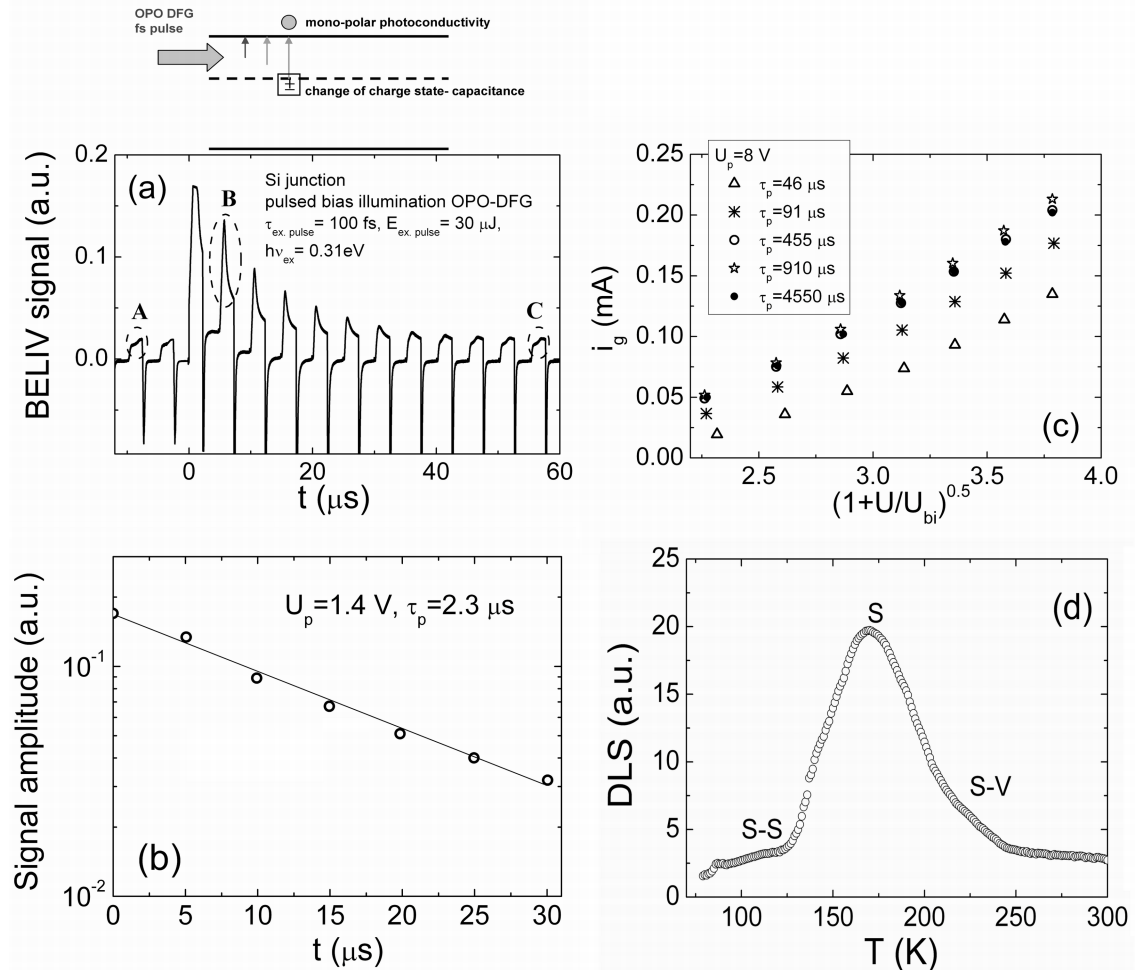


**Figure 3.** a- A sequence of BCC transients measured in a Si thyristor junction structure. **A** indicates a typical transient determined by carrier capture into deep traps before IR illumination pulse, **B** shows a modified BCC transient just after IR illumination ( $\lambda = 4 \mu\text{m}$ ) by 100 fs pulse, and **C** illustrates the recovered BCC transient after photo-ionized carriers are re-trapped by deep centres. In the inset (i), a sketch of the photo-ionization processes is presented. b- Relaxation of the initial amplitude of the B-type transients within semilog scale and evaluation of the carrier recombination/capture lifetime. c- Generation current as a function of  $(1 + U(t)/U_{bi})^{1/2}$  and LIV pulse duration. d- C-DLTS spectrum measured in the Si thyristor junction structure. The DLTS peak ascribed to a single charged sulphur (S) dominates, and  $S_i-S_s$  as well as sulphur vacancy (S-V) associated peaks, interpreted according to [10]–[12], are also denoted.

illumination, whereby the generation (leakage) current dominates over the barrier capacitance current for GLIV pulse durations of  $\tau_p > 1 \mu\text{s}$ . To verify the existence of defects in the n-base region and to identify the traps responsible for the generation current, C-DLTS spectra have also been recorded on the same device structures (figure 3d). The prevailing peak in the range of 150–200 K is obtained in the C-DLTS spectrum which is ascribed to the sulphur contaminant impurities [10]–[12] with activation energy of 0.3 eV and cross-section of  $\sigma \sim 5 \times 10^{-16} \text{ cm}^2$ . Due to high density of technological contaminants, only qualitative evaluation of trap concentration and other DLTS signatures is possible when trap density approaches to or exceeds the doping density.



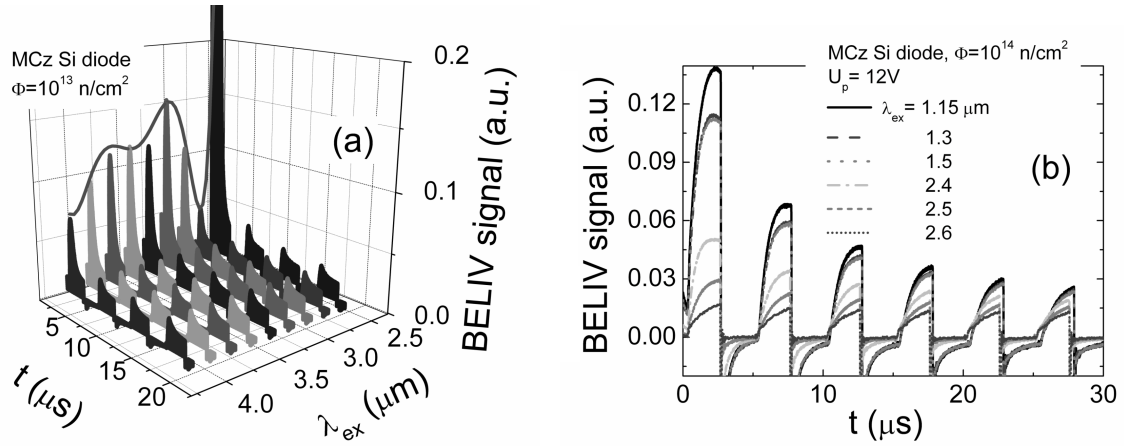


**Figure 4.** BCC transients as a function of wavelength and time measured in Si pin detector structures irradiated with  $10^{13}$  (a) and  $10^{14}$  (b)  $\text{n/cm}^2$  reactor neutrons fluence.

The obtained DLTS spectra actually corroborated the existence of deep traps as revealed by the BELIV-IR spectroscopy measurements. Our results illustrates that the proposed BELIV-IR pulsed spectroscopy technique permits time resolved spectroscopy with the simultaneous determination of carrier capture and emission lifetimes. Calibration of the illumination density at each wavelength (simultaneously measured in our experiments) would enable to determine the concentration of each of the deep traps resolved as a spectral peak in the n-layer of the  $\text{n}^+\text{pnp}$  structures.

## 5 Illumination spectrum dependent BELIV current transients in the irradiated diodes

Prevailing of the barrier charging current (figure 4a) has been observed in Si pin detectors irradiated with a rather low fluence of reactor neutrons ( $\Phi \leq 10^{13} \text{ n/cm}^2$ ). The photo-ionization peaks probed by BELIV current are determined varying illumination quanta  $h\nu$ .

The evolution of the BCC transients, illustrated in figure 4a, as a function of the illumination wavelength for the same quanta flux (calibrated OPO-DFG energy per pulse) shows photo-ionization peaks with activation energy values of  $E_1 = 0.3 \pm 0.02 \text{ eV}$ ,  $E_2 = 0.41 \pm 0.01 \text{ eV}$  and  $E_3 = 0.51 \pm 0.01 \text{ eV}$  in an n-Si layer with a dopant density of  $N_D \approx 10^{12} \text{ cm}^{-3}$  irradiated with  $\Phi = 10^{13} \text{ n/cm}^2$ . Best fit of these peaks, simulated by using eqs. (2.1)–(2.5) (and  $[N_D - (N_{AT} - n_T(t))]$  when necessary, with  $N_{AT}$  the density of acceptor-type traps) can be associated with well-known [13] deep centres ascribed to radiation defects. In figure 4a, it can also be noticed, that the capture lifetime varies for different deep traps, as deduced from the BCC amplitude reduction rate within a sequence of transients at fixed illumination wavelength.

In Si pin detectors irradiated with  $\Phi \geq 10^{14} \text{ n/cm}^2$  fluence, when the deep trap density exceeds that of the shallow dopants, the generation current  $i_{gl}$  dominates in the BCC transients, even when using the highest illumination density of the OPO-DFG source, being the IR spectrum brightest laser, and rather short LIV pulses. The evolution of the BCC transients shown in figure 4b can be explained by a simultaneous increase of the SC generation current ( $i_{gl}$ ) and of the dielectric



relaxation time. This leads to an increase of series resistance of the ENR n-Si region. A high density of deep traps also leads to a partial filling of the different deep centres due to a lack of “native” equilibrium carriers which is determined by the shallow dopants of low ( $N_D \approx 10^{12} \text{ cm}^{-3}$ ) concentration. Then, deep traps characterized by the longest carrier emission lifetime (i.e. the deepest centres) which exceeds the carrier capture lifetime can be filled [6]. This prediction is proven in our experiments on the Si pin detectors heavily irradiated with neutron fluences in the range of  $\Phi = 10^{14}$  to  $10^{16} \text{ n/cm}^2$ , when a threshold for photo-ionization is observed for quanta of energy  $h\nu \geq 0.5 \text{ eV}$ . The BELIV-IR spectral peak revealed in figure 4b can only be obtained for an OPO illumination wavelength of  $\lambda \cong 1.2 \mu\text{m}$ , which is close to the inter-band excess carrier photo-generation. This illustrates that the BELIV-IR spectroscopy technique is applicable even in the case of a high density of traps.

One of the limiting factors in extracting the activation energy value (when using threshold wavelength for photo-ionization of definite traps) is spectral width  $\Delta(h\nu)$  of OPO radiation. The spectral broadening of fs pulsed radiation is about  $\Delta(h\nu) = 10\text{--}80 \text{ meV}$ , and this broadening increases with wavelength. However, at room temperature, relatively shallow levels are thermally ionized, and  $\Delta(h\nu)/h\nu \cong 2\text{--}20 \%$  for the observed peaks. OPO pulses of ps duration are preferential to reduce spectral broadening of tuneable wavelength IR illumination. Actually, illumination at peak wavelength dominates within photo-ionization of trapped carriers when using fs pulses. The BELIV-IR spectroscopy technique is preferential when traditionally used methods (e.g. TSC – thermally stimulated currents at 300 K and DLTS at high density of several species traps in samples with large leakage currents) are non-operational.

## 6 Summary

In summary, the proposed BELIV-IR pulsed spectroscopy technique can be used as a powerful tool for the examination of deep levels in the junction area of semiconductor device structures even when a high density of defects is present. This technique allows for the simultaneous measurements of the excess carrier capture and short emission lifetime within the resistive junction layer of a semiconductor device structure. Spectra measured by the BELIV-IR pulsed technique have been compared with those registered by C-DLTS on the same Si thyristor structures in the case that the dopant density is close to that of the trap concentration showing good agreement between both techniques. One of the additional advantages of the BELIV-IR technique is that it can be performed at room temperature which is closer to the real operation of the devices and without the need for temperature scanning in a cryostat.

## Acknowledgments

J. Vanhellemont is acknowledged for help in edition of the text and useful suggestions. G. Kramberger is appreciated for providing the irradiated samples. This research was funded by a grant MIP-54/2011 from the Research Council of Lithuania.

## References

- [1] P. Blood and J.W. Orton, *The electrical characterization of semiconductors: majority carriers and electron states*, Academic Press, U.S.A. (1992).
- [2] N. Shashank, V. Singh, S.K. Gupta, K.V. Madhu, J. Akhtar and R. Damle, *DLTS and in situ C–V analysis of trap parameters in swift 50 MeV Li<sup>3+</sup> ion-irradiated Ni/SiO<sub>2</sub>/Si MOS capacitors*, *Radiat. Eff. Defect. S.* **166** (2011) 313.
- [3] Z. Li and C.J. Li, *Development of current-based microscopic defect analysis method using optical filling techniques for the defect study on heavily irradiated high-resistivity Si sensors/detectors*, *Mat. Sci. Semicon. Proc.* **9** (2006) 283.
- [4] S.T. Pantelides, *The electronic structure of impurities and other point defects in semiconductors*, *Rev. Mod. Phys.* **50** (1978) 797.
- [5] E. Gaubas, T. Ceponis and J. Vaitkus, *Impact of generation current on the evaluation of the depletion width in heavily irradiated Si detectors*, *J. Appl. Phys.* **110** (2011) 033719.
- [6] E. Gaubas, T. Ceponis, J. Kusakovskij, *Profiling of barrier capacitance and spreading resistance using a transient linearly increasing voltage technique*, *Rev. Sci. Instr.* **82** (2011) 083304.
- [7] T. Ceponis et al., *In situ analysis of carrier lifetime and barrier capacitance variations in silicon during 1.5 MeV protons implantation*, [2011 JINST 6 P09002](#).
- [8] G. Lucovsky, *On the photoionization of deep impurity centers in semiconductors*, *Solid State Commun.* **3** (1965) 299.
- [9] E. Gaubas, A. Uleckas, R. Grigonis, V. Sirutkaitis and J. Vanhellemon, *Microwave probed photoconductivity spectroscopy of deep levels in Ni doped Ge*, *Appl. Phys. Lett.* **92** (2008) 222102.
- [10] H.G. Grimmeiss, *Deep level impurities in semiconductors*, *Annu. Rev. Mater. Sci.* **7** (1977) 341.
- [11] J.W. Chen and A.G. Milnes, *Energy levels in silicon*, *Annu. Rev. Mater. Sci.* **10** (1980) 157.
- [12] M. Karimov and A. Karakhodzhaev, *Influence of the post-diffusion hardening rate and thermal treatment on the thermal stability of the charge-carrier lifetime in overcompensated n-Si(B,S)*, *Russ. Phys. J.* **44** (2001) 734.
- [13] M. Huhtinen, *Simulation of non ionising energy loss and defect formation in silicon*, *Nucl. Inst. Meth.* **A 491** (2002) 194.